Supporting Information

Impact of Heat on Coil Hydrodynamic Size Yields the Energetics of Denatured State Conformational Bias

Lance R. English,[1,2] Sarah M. Voss,[1] Erin C. Tilton,[1] Elisia A. Paiz,[1] Stephen So,[1] George L. Parra,[1] Steven T. Whitten*[1]

[1]Department of Chemistry and Biochemistry, Texas State University, San Marcos, Texas 78666, United States
[2]Department of Biology, Texas State University, San Marcos, Texas 78666, United States

Supporting Tables

Table S1. IDP database.

Protein	mean R_h[a]	Q_{net}[b]	f_{PPII}[c]	f_{PPII}[d]	f_{PPII}[e]	Primary Sequence
abeta (1-40)	14.4	3	0.304	0.340	0.320	DAEFRHDSGY EVHHQKLVFF AEDVGSNKGA IIGLMVGGVV
α-synuclein	28.2	9	0.374	0.363	0.334	MDVFMKGLSK AKEGVVAAAE KTKQGVAEAA GKTKEGVLYV GSKTKEGVVH GVATVAEKTK EQVTNVGGAV VTGVTAVAQK TVEGAGSIAA ATGFVKKDQL GKNEEGAPQE GILEDMPVDP DNEAYEMPSE EGYQDYEPEA
Cad136	28.1	9	0.402	0.385	0.360	RLEQYTSAVV GNKAAKPAKP AASDLPVPAE GVRNIKSMWE KGNVFSSPGG TGTPNKETAG LKVGVSSRIN EWLTKTPEGN KSPAPKPSDL RPGDVSGKRN LWEKQSVEKP AASSSKVTAT GKKSETNGLR QFEKEP
CFTR-R-region	32.0	5	0.364	0.369	0.343	GAMESAERRN SILTETLHRF SLEGDAPVSW TETKKQSFKQ TGEFGEKRKN SILNPINSIR KFSIVQKTPL QMNGIEEDSD EPLERRLSLV PDSEQGEAIL PRISVISTGP TLQARRRQSV LNLMTHSVNQ GQNIHRKTTA STRKVSLAPQ ANLTELDIYS RRLSQETGLE ISEEINEEDL KECLFDDME
Fos-AD	35.0	16	0.378	0.406	0.369	GSHMSVASLD LTGGLPEVAT PESEEAFTLP LLNDPEPKPS VEPVKSISSM ELKTEPFDDF LFPASSRPSG SETARSVPDM DLSGSFYAAD WEPLHSGSLG MGPMATELEP LCTPVVTCTP SCTAYTSSFV FTYPEADSFP SCAAAHRKGS SSNEPSSDSL SSPTLLAL
Hdm2-ABD	31.7	29	0.335	0.359	0.334	ERSSSSESTG TPSNPDLDAG VSEHSGDWLD QDSVSDQFSV EFEVESLDSE DYSLSEEGQE LSDEDDEVYQ VTVYQAGESD TDSFEEDPEI SLADYWK
HIF1-α-403	44.3	29	0.402	0.411	0.392	PAAGDTIISL DFGSNDTETD DQQLEEVPLY NDVMLPSPNE KLQNINLAMS PLPTAETPKP LRSSADPALN QEVALKLEPN PESLELSFTM PQIQDQTPSP SDGSTRQSSP EPNSPSEYCF YVDSDMVNEF KLELVEKLFA EDTEAKNPFS TQDTDLDLEM LAPYIPMDDD FQLRSFDQLS PLESSSASPE SASPQSTVTV FQ
HIF1-α-530	38.3	10	0.390	0.384	0.367	NEFKLELVEK LFAEDTEAKN PFSTQDTDLD LEMLAPYIPM DDDFQLRSFD QLSPLESSSA SPESASPQST VTVFQQTQIQ EPTANATTTT ATTDELKTVT KDRMEDIKIL IASPSPTHIH KETTSATSSP YRDTQSRTAS PNRAGKGVIE QTEKSHPRSP NVLSVALSQR
LJIDP1	24.5	4	0.356	0.371	0.324	MARSFTNIKA ISALVAEEFS NSLARRGYAA TAQSAGRVGA SMSGKMGSTK SGEEKAAARE KVSWVPDPVT GYYKPENIKE IDVAELRSAV LGKN
Mlph (147-240)	28.0	15	0.353	0.371	0.335	RLQGGGGSEP SLEEGNGDSE QTDEDGDLDT EARDQPLNSK KKKRLLSFRD VDFEEDSDHL VQPCSQTLGL SSVPESAHSL QSLSGEPYSE DTTSLEP

Protein	mean R_h[a]	Q_{net}[b]	f_{PPII}[c]	f_{PPII}[d]	f_{PPII}[e]	Primary Sequence
Mlph (147-403)	49.0	28	0.370	0.382	0.347	RLQGGGGSEP SLEEGNGDSE QTDEDGDLDT EARDQPLNSK KKKRLLSFRD VDFEEDSDHL VQPCSQTLGL SSVPESAHSL QSLSGEPYSE DTTSLEPEGL EETGARALGC RPSPEVQPCS PLPSGEDAHA ELDSPAASCK SAFGTTAMPG TDDVRGKHLP SQYLADVDTS DEDSIQGPRA ASQHSKRRAR TVPETQILEL NKRMSAVEHL LVHLENTVLP PSAQEPTVET HPSADTEEET LRRRLEELTS NISGSSTSSE
p53 ALA-rich mutant	32.5	15	0.495	0.488	0.454	GMEEPQSDPS AEPPASQETA SDAWKALPEN NALSPLPSQA ADDAMASPDD AEQAFTEDPG PDEAPRMPEA APPAAPAPAA PTPAAPAPAP SWPL
p53 GLY-rich mutant	30.7	15	0.456	0.445	0.421	GMEEPQSDPS GEPPGSQETG SDGWKGLPEN NGLSPLPSQA GDDGMGSPDD GEQGFTEDPG PDEAPRMPEG APPGAPAPGA PTPGAPAPAP SWPL
p53 ILE-rich mutant	33.3	15	0.498	0.474	0.494	GMEEPQSDPS IEPPISQETI SDIWKILPEN NILSPLPSQA IDDIMISPDD IEQIFTEDPG PDEAPRMPEI APPIAPAPIA PTPIAPAPAP SWPL
p53 LEU-rich mutant	33.1	15	0.474	0.486	0.466	GMEEPQSDPS LEPPLSQETL SDLWKLLPEN NLLSPLPSQA LDDLMLSPDD LEQLFTEDPG PDEAPRMPEL APPLAPAPLA PTPLAPAPAP SWPL
p53 MET-rich mutant	32.0	15	0.493	0.472	0.444	GMEEPQSDPS MEPPMSQETM SDMWKMLPEN NMLSPLPSQA MDDMMMSPDD MEQMFTEDPG PDEAPRMPEM APPMAPAPMA PTPMAPAPAP SWPL
p53 PRO-rich mutant	33.7	15	0.595	0.541	0.551	GMEEPQSDPS PEPPPSQETP SDPWKPLPEN NPLSPLPSQA PDDPMPSPDD PEQPFTEDPG PDEAPRMPEP APPPAPAPPA PTPPAPAPAP SWPL
p53 VAL-rich mutant	33.4	15	0.498	0.466	0.484	GMEEPQSDPS VEPPVSQETV SDVWKVLPEN NVLSPLPSQA VDDVMVSPDD VEQVFTEDPG PDEAPRMPEV APPVAPAPVA PTPVAPAPAP SWPL
p53 (1-93) wildtype	32.4	15	0.482	0.477	0.464	GSMEEPQSDP SVEPPLSQET FSDLWKLLPE NNVLSPLPSQ AMDDLMLSPD DIEQWFTEDP GPDEAPRMPE AAPPVAPAPA APTPAAPAPA PSWPL
p53 (1-93) ALA^-	30.4	15	0.452	0.442	0.438	GSMEEPQSDP SVEPPLSQET FSDLWKLLPE NNVLSPLPSQ GMDDLMLSPD DIEQWFTEDP GPDEGPRMPE GGPPVGPGPG GPTPGGPGPG PSWPL
p53 (1-93) ALA^- PRO^-	27.4	15	0.251	0.303	0.248	GSMEEGQSDG SVEGGLSQET FSDLWKLLGE NNVLSGLGSQ GMDDLMLSGD DIEQWFTEDG GGDEGGRMGE GGGGVGGGGG GGTGGGGGGG GSWGL
p53 (1-93) PRO^-	27.5	15	0.281	0.338	0.275	GSMEEGQSDG SVEGGLSQET FSDLWKLLGE NNVLSGLGSQ AMDDLMLSGD DIEQWFTEDG GGDEAGRMGE AAGGVAGAGA AGTGAAGAGA GSWGL

Protein	mean R_h[a]	Q_{net}[b]	f_{PPII}[c]	f_{PPII}[d]	f_{PPII}[e]	Primary Sequence
p53-TAD	23.8	14	0.450	0.446	0.437	MEEPQSDPSV EPPLSQETFS DLWKLLPENN VLSPLPSQAM DDLMLSPDDI EQWFTEDPGP DEAPRMPEAA PRV
p57-ID	24.0	6	0.364	0.380	0.355	VRTSACRSLF GPVDHEELSR ELQARLAELN AEDQNRWDYD FQQDMPLRGP GRLQWTEVDS DSVPAFYRET VQV
PDE-γ	24.8	4	0.412	0.394	0.383	MNLEPPKAEI RSATRVMGGP VTPRKGPPKF KQRQTRQFKS KPPKKGVQGF GDDIPGMEGL GTDITVICPW EAFNHLELHE LAQYGII
PGR	37.7	7	0.535	0.477	0.451	AEPGKPAEPG KPAEPGKPAE PGTPAEPGKP AEPGTPAEPG KPAEPGKPAE PGKPAEPGKP AEPGTPAEPG TPAEPGKPAE PGTPAEPGKP AEPGTPAEPG KPAESGKPVE PGTPAQSGAP EQPNRSMHST DNKNQ
prothymosin-α	33.6	43	0.363	0.354	0.317	MSDAAVDTSS EITTKDLKEK KEVVEEAENG RDAPANGNAN EENGEQEADN EVDEEEEEGG EEEEEEEEGD GEEEDGDEDE EAESATGKRA AEDDEDDDVD TKKQKTDEDD
Retro-nuclease	34.0	8	0.379	0.370	0.342	GQGSDANDES WINLKEKKAQ AESKRLHQEH TNNPKYVYAV KALGQRVLAE NVMKGDAYIY ALGRGYKDTR QGKDFEVEIK KANEVMKKTF ASAEPGYKEV GKKPHKTEPT DVLLLRFTMP QGKYMLKVTD GDIAKILTAP EKHLKKTSAT
Securin	39.7	1	0.413	0.410	0.394	MATLIYVDKE NGEPGTRVVA KDGLKLGSGP SIKALDGRSQ VSTPRFGKTF DAPPALPKAT RKALGTVNRA TEKSVKTKGP LKQKQPSFSA KKMTEKTVKA KSSVPASDDA YPEIEKFFPF NPLDFESFDL PEEHQIAHLP LSGVPLMILD EERELEKLFQ LGPPSPVKMP SPPWESNLLQ SPSSILSTLD VELPPVCCDI DI
ShB-C	32.9	4	0.376	0.363	0.329	MTLGQHMKKS SLSESSSDMM DLDDGVESTP GLTETHPGRS AVAPFLGAQQ QQQQPVASSL SMSIDKQLQH PLQQLTQTQL YQQQQQQQQQ QQNGFKQQQQ QTQQQLQQQQ SHTINASAAA ATSGSGSSGL TMRHNNALAV SIETDV
sml1	23.4	5	0.363	0.375	0.330	MQNSQDYFYA QNRCQQQQAP STLRTVTMAE FRRVPLPPMA EVPMLSTQNS MGSSASASAS SLEMWEKDLE ERLNSIDHDM NNNKFGSGEL KSMFNQGKVE EMDF
SNAP25	39.7	14	0.351	0.360	0.325	MAEDADMRNE LEEMQRRADQ LADESLESTR RMLQLVEESK DAGIRTLVML DEQGEQLERI EEGMDQINKD MKEAEKNLTD LGKFCGLCVC PCNKLKSSDA YKKAWGNNQD GVVASQPARV VDEREQMAIS GGFIRRVTND ARENEMDENL EQVSGIIGNL RHMALDMGNE IDTQNRQIDR IMEKADSNKT RIDEANQRAT KMLGSG
Tau-K45	45.0	19	0.399	0.376	0.368	MSSPGSPGTP GSRSRTPSLP TPPTREPKKV AVVRTPPKSP SSAKSRLQTA PVPMPDLKNV KSKIGSTENL KHQPGGGKVQ IINKKLDLSN VQSKCGSKDN IKHVPGGGSV QIVYKPVDLS KVTSKCGSLG NIHHKPGGGQ VEVKSEKLDF KDRVQSKIGS LDNITHVPGG GNKKIETHKL TFRENAKAKT DHGAEIVY

Protein	mean R_h[a]	Q_{net}[b]	f_{PPII}[c]	f_{PPII}[d]	f_{PPII}[e]	Primary Sequence
Vmw65	28.0	19	0.328	0.379	0.347	GSAGHTRRLS TAPPTDVSLG DELHLDGEDV AMAHADALDD FDLDMLGDGD SPGPGFTPHD SAPYGALDMA DFEFEQMFTD ALGIDEYGG

[a] experimental mean R_h (in Å) from literature reports[1,2] except for the p53(1-93) substitution mutants that were measured in the current study. For these mutants, the SEC and DLS average is given.
[b] Q_{net} calculated from the primary sequence as the absolute value of number of LYS and ARG residues minus the number of GLU and ASP
[c] f_{PPII} calculated from the primary sequence by $\sum P_{PPII,I} / N$, where $P_{PPII,i}$ is the PPII propensity for amino acid type i using the peptide scale[3]
[d] f_{PPII} calculated from the primary sequence by $\sum P_{PPII,I} / N$, where $P_{PPII,i}$ is the PPII propensity for amino acid type i using the coil library scale[4]
[e] f_{PPII} calculated from the primary sequence by $\sum P_{PPII,I} / N$, where $P_{PPII,i}$ is the PPII propensity for amino acid type i using the IDP scale, which was determined in the current study (see Table S2)

Table S2. Amino acid specific propensities for the PPII conformation (± standard deviation, where available) in the denatured state.

Amino Acid	IDP scale[a]	coil library scale[b]	peptide scale[c]	peptide scale[d]	peptide scale[e]
ALA (A)	0.32 ± 0.05	0.48 ± 0.02	0.37 ± 0.03	0.818	0.61 ± 0.02
CYS (C)	0.22 ± 0.04	0.38 ± 0.04	0.25 ± 0.02	0.557	0.55 ± 0.02
ASP (D)	0.44 ± 0.07	0.34 ± 0.02	0.30 ± 0.02	0.552	0.63 ± 0.02
GLU (E)	0.27 ± 0.04	0.38 ± 0.02	0.42 ± 0.03	0.684	0.61 ± 0.02
PHE (F)	0.31 ± 0.07	0.36 ± 0.03	0.17 ± 0.01	0.639	0.58 ± 0.02
GLY (G)	0.11 ± 0.01	0.21 ± 0.01	0.13 ± 0.01	-	0.58 ± 0.02
HIS (H)	0.23 ± 0.04	0.28 ± 0.03	0.20 ± 0.01	0.428	0.55 ± 0.02
ILE (I)	0.57 ± 0.07	0.39 ± 0.02	0.39 ± 0.03	0.519	0.50 ± 0.01
LYS (K)	0.33 ± 0.06	0.35 ± 0.02	0.56 ± 0.04	0.581	0.59 ± 0.02
LEU (L)	0.39 ± 0.06	0.47 ± 0.02	0.24 ± 0.02	0.574	0.58 ± 0.02
MET (M)	0.25 ± 0.05	0.38 ± 0.04	0.36 ± 0.02	0.498	0.55 ± 0.02
ASN (N)	0.29 ± 0.09	0.31 ± 0.02	0.27 ± 0.02	0.667	0.55 ± 0.02
PRO (P)	0.93 ± 0.01	0.81 ± 0.01	1.00	-	0.67 ± 0.02
GLN (Q)	0.35 ± 0.08	0.35 ± 0.02	0.53 ± 0.04	0.654	0.66 ± 0.02
ARG (R)	0.26 ± 0.04	0.32 ± 0.02	0.38 ± 0.03	0.638	0.61 ± 0.02
SER (S)	0.21 ± 0.03	0.31 ± 0.02	0.24 ± 0.02	0.774	0.58 ± 0.02
THR (T)	0.28 ± 0.07	0.24 ± 0.02	0.32 ± 0.02	0.553	0.53 ± 0.01
VAL (V)	0.50 ± 0.07	0.34 ± 0.02	0.39 ± 0.03	0.743	0.49 ± 0.01
TRP (W)	0.42 ± 0.12	0.35 ± 0.04	0.25 ± 0.01	0.764	-
TYR (Y)	0.27 ± 0.05	0.37 ± 0.03	0.25 ± 0.01	0.630	-

[a] determined from the sequence dependence to IDP mean R_h analyzed in the current study; these values were calculated from the average of the "best" random scales (with error cut-off of 0.165) that maintained the P>V~I>L>A>M>G rank order.
[b] determined from PPII frequencies in the protein coil library[4]
[c] determined from host-guest analysis of the binding energetics of the Sos peptide[3]
[d] determined from 3-bond coupling constants measured for a glycine-based host peptide[5]
[e] determined from CD spectra measured for a proline-based host peptide[6]

Supporting Figures

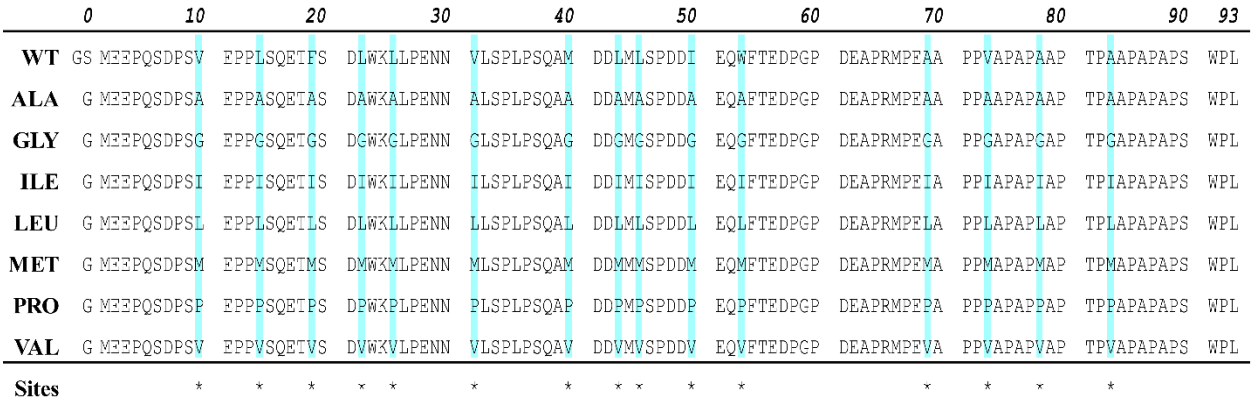

Figure S1. Primary sequences of the p53(1-93) substitution mutants used in the current study. Mutant identity is given in the left-most column by the 3-letter amino acid code representing the substitution. WT is the wild type variant of the p53(1-93) fragment. Substitution sites are marked by an asterisk and highlighted blue.

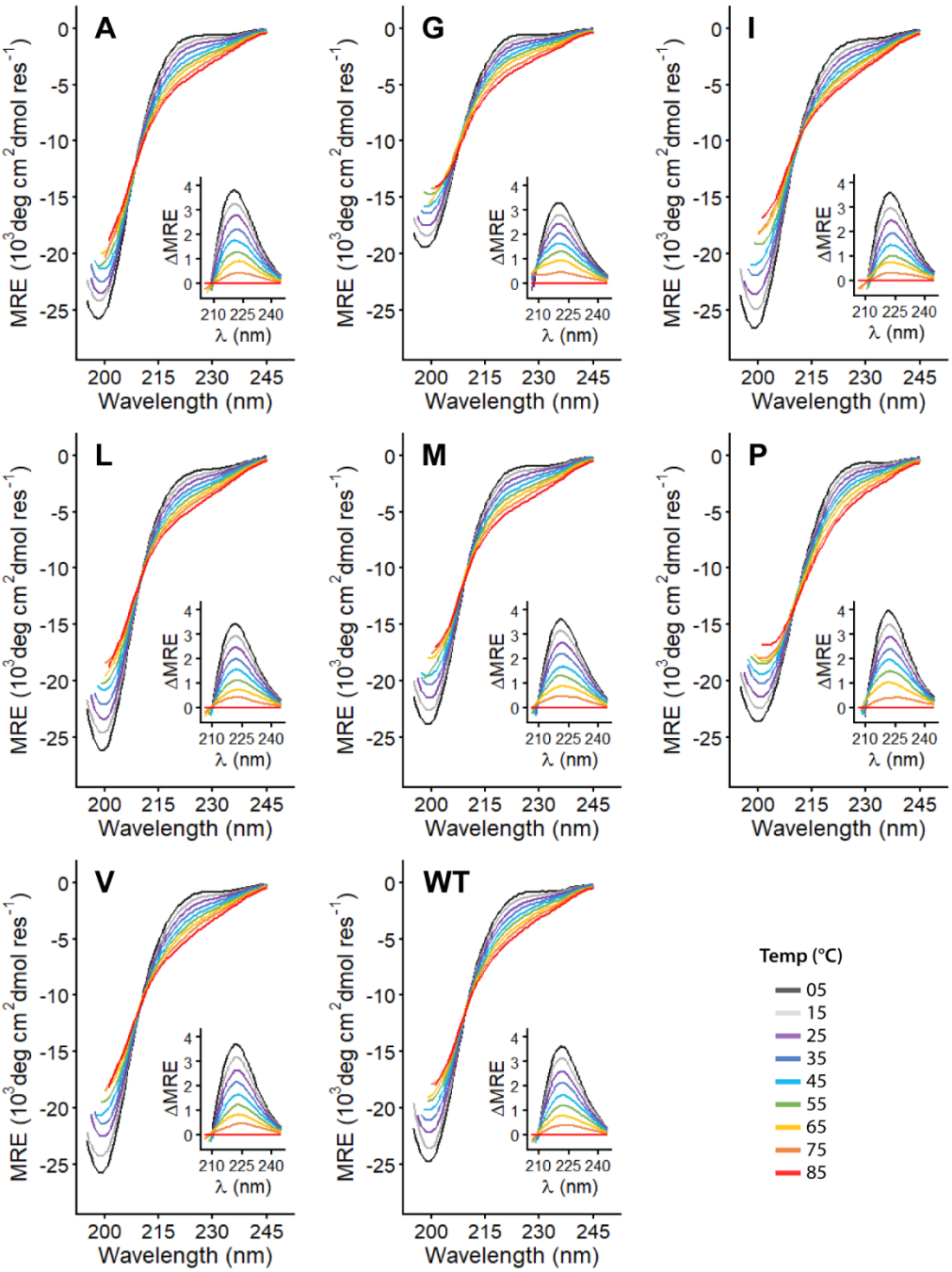

Figure S2. Temperature dependence to the CD spectrum of the p53(1-93) substitution mutants. Inset figures show the difference spectrum relative to the 85°C spectrum. Mutant identity is given in the upper left of each plot by the 1-letter amino acid code representing the substitution. WT is the wild type variant of the p53(1-93) fragment.

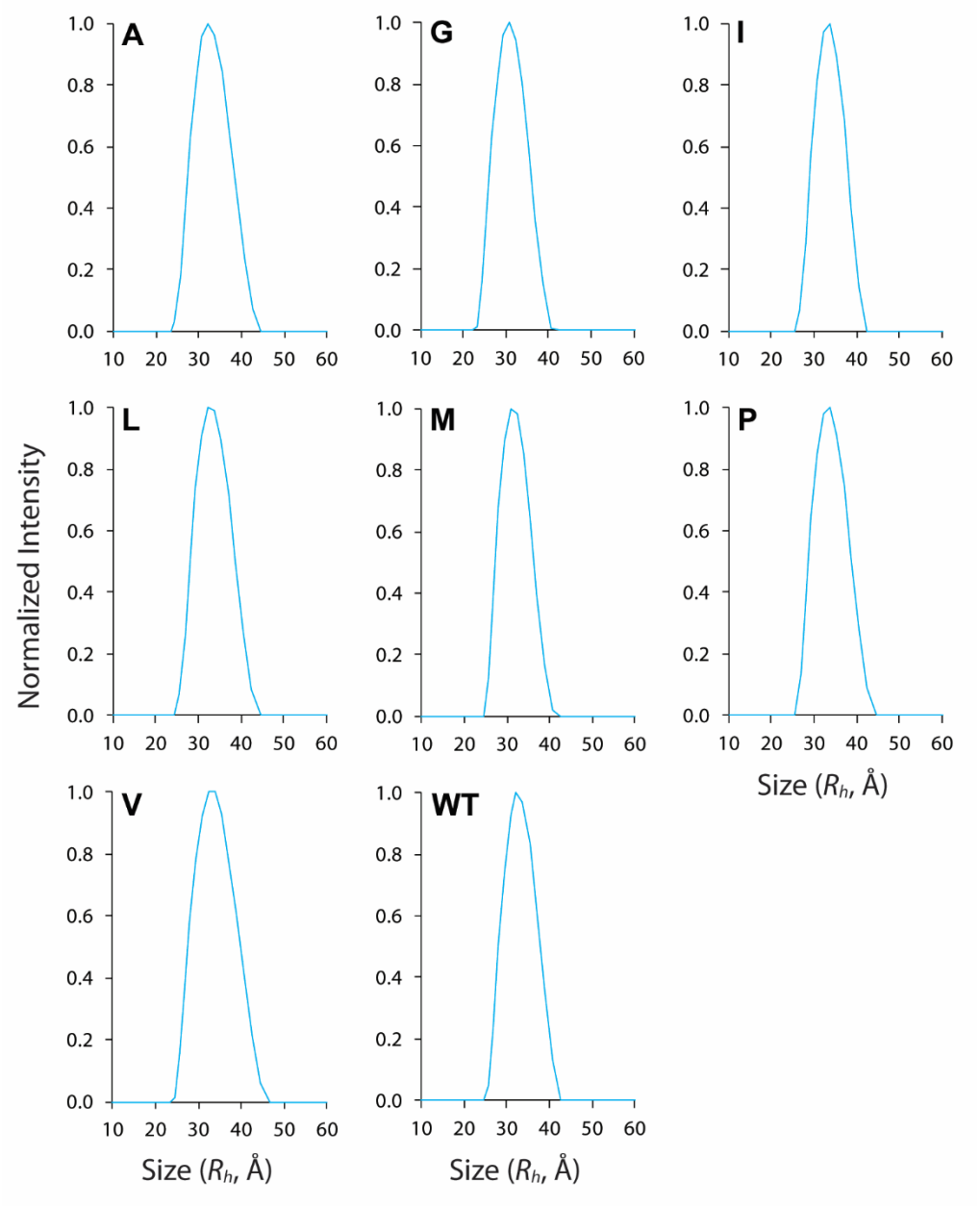

Figure S3. DLS-measured size distributions of the p53(1-93) substitution mutants. Shown are representative size distributions that were measured at 25°C for each mutant. Mutant identity is given in the upper left of each plot by the 1-letter amino acid code representing the substitution. WT is the wild type variant of the p53(1-93) fragment.

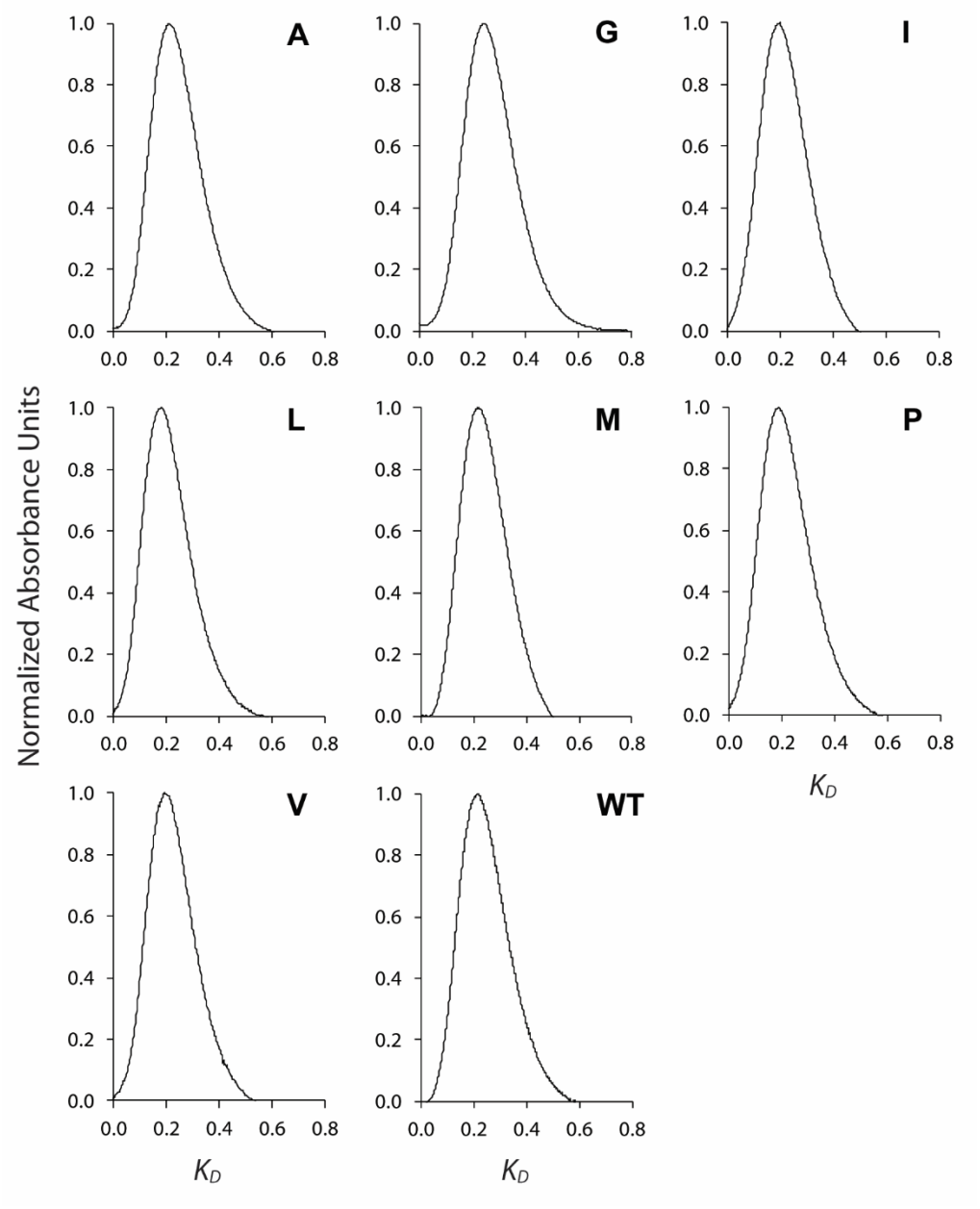

Figure S4. SEC-measured size chromatograms of the p53(1-93) substitution mutants. Shown are representative chromatograms that were measured at room temperature, ~23°C. Mutant identity is given in the upper right of each plot by the 1-letter amino acid code representing the substitution. WT is the wild type variant of the p53(1-93) fragment.

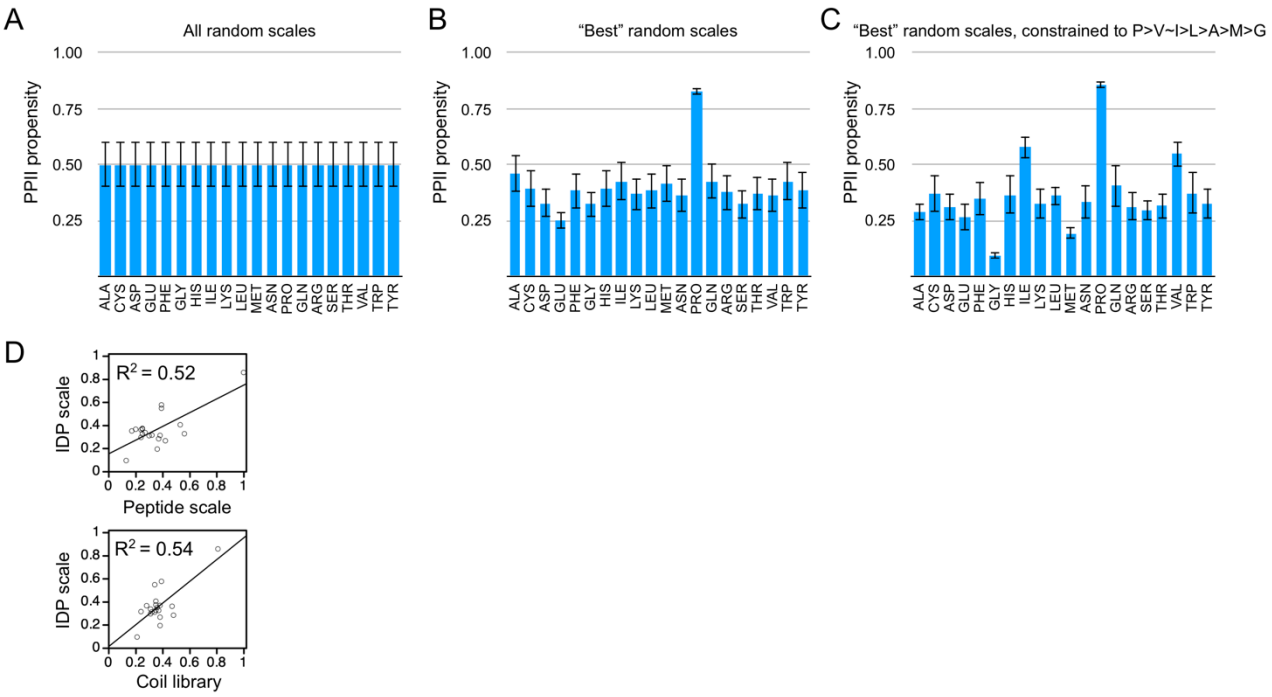

Figure S5. Amino acid average scale propensity calculated from randomly generated PPII scales. Calculated from **A)** all random scales, **B)** the "best" scales, and **C)** the "best" scales that maintain the P>V~I>L>A>M>G rank order. In panels A-C, error bars are the standard deviations associated with the averages. In panels B and C, the "best" scales that were used had an error threshold of 0.2. **D)** Linear correlation of the peptide and IDP scales (top), and the coil library and IDP scales (bottom), using the panel C values for the IDP scale.

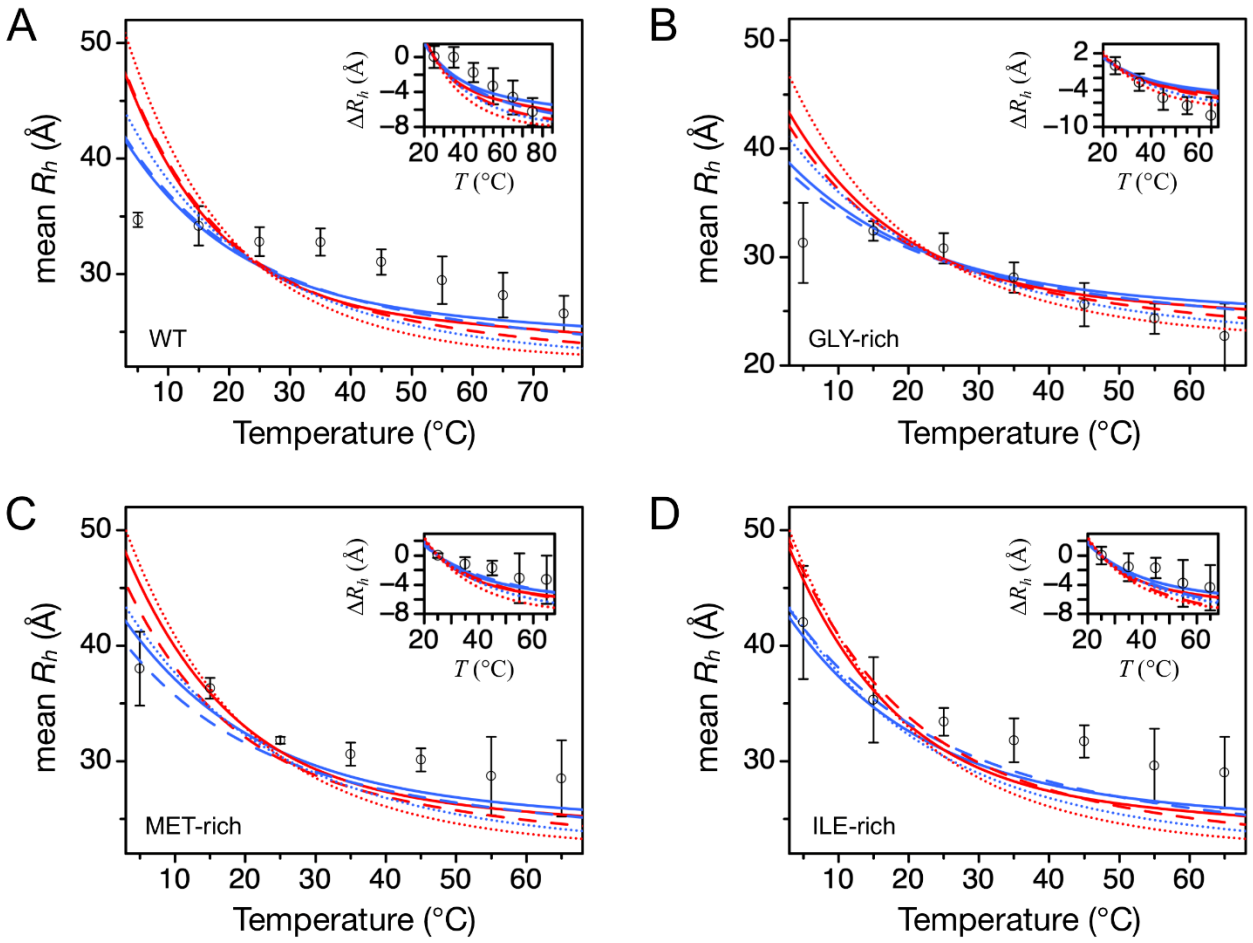

Figure S6. Temperature dependence to mean R_h for the p53(1-93) substitution mutants. Representative data are provided for the wild type (WT) and three substitution mutants. WT DLS results are from.[7] DLS readings for the p53(1-93) proteins generally gave low count rates, causing long read times, which compromised the measurements at the temperature extremes; by condensation on the cuvette at cold temperatures and sample evaporation at high temperatures. Note the large uncertainties in the measurements. In the figure and each inset, lines were calculated using each protein's primary sequence. Blue lines used 10 kcal mol^{-1} for ΔH_{PPII}, while red used 13 kcal mol^{-1}. Solid lines used the peptide scale to calculate f_{PPII}, stippled lines the coil library scale, and dashed lines the IDP scale. Open circles are mean R_h measured by DLS. Error bars are the standard deviations in the measurements. Inset shows change in mean R_h (ΔR_h) relative to the 25°C value.

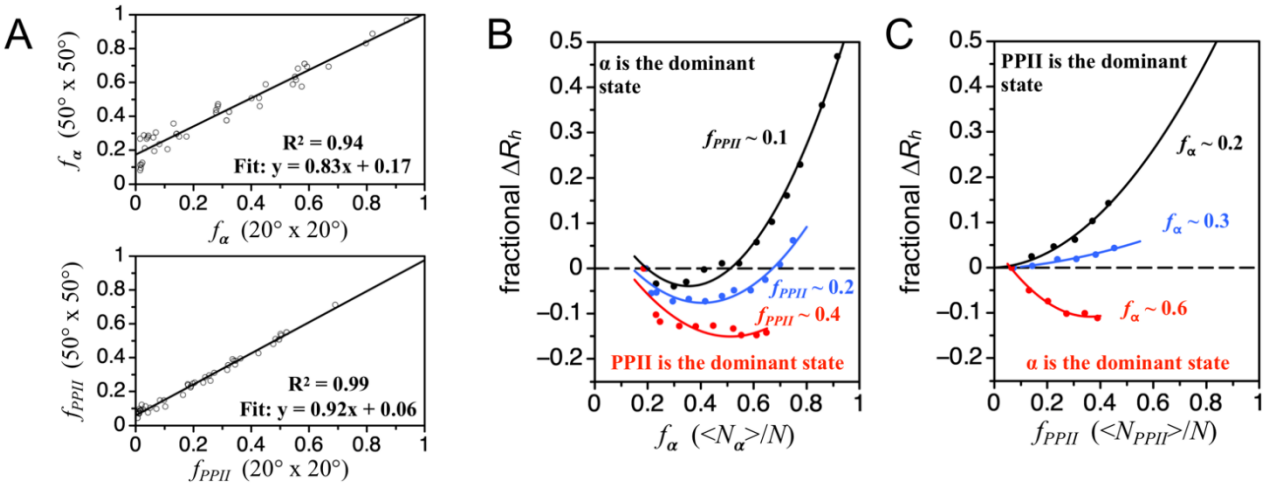

Figure S7. Simulation of the R_h dependence on the α and PPII bias. Ensembles of random polyalanine conformers were generated by computer algorithm using the HSC model[7–9], whereby dihedral angles (φ, ψ) for each residue were assigned randomly. The goal was to compute the mean size for an ensemble and then establish how the mean size changes when an artificial bias to the α or PPII regions, or to both regions, is applied.[1,7,9] Figure 5 in the main text shows the results from defining the α and PPII regions as (-64°±10°, -41°±10°) and (-75°±10°, +145°±10°), respectively. Results shown here were obtained by increasing the α and PPII regions to (-64°±25°, -41°±25°) and (-75°±25°, +145°±25°), respectively. Each open or closed circle represents a simulated 25-residue polyalanine ensemble. Lines are fits; linear in panel A and 2nd order polynomials in panels B and C. **A)** Across many ensembles, f_α and f_{PPII} defined by the smaller, 20°x20° regions correlated with f_α and f_{PPII} calculated using larger, 50°x50° regions. Consequently, the trends in α and PPII effects on R_h should remain mostly unchanged when the extent of the α and PPII regions is increased. Consistent with that idea, when defining α and PPII by the larger 50°x50° regions, ensemble simulations again showed that **B)** increased PPII bias causes increased sensitivity to changes in f_α, and **C)** increasing the α bias suppresses the PPII effect on R_h and, when α is the dominant state, reverses the PPII effect.

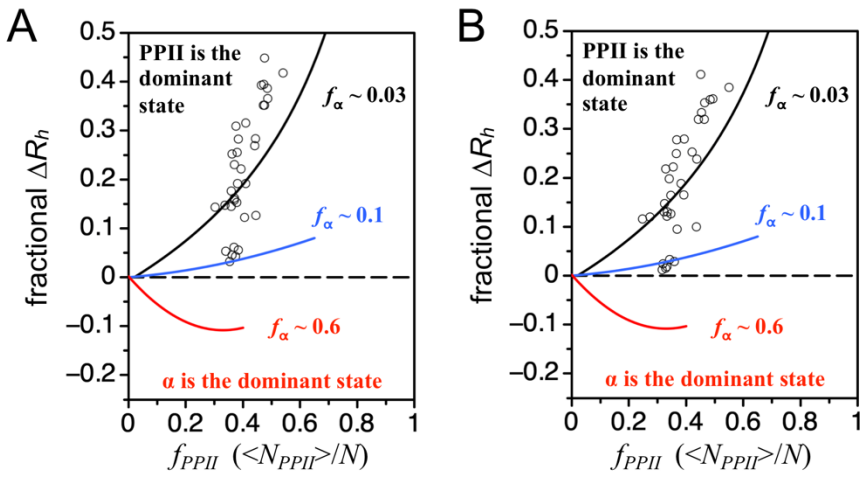

Figure S8. Simulation of the R_h dependence on the α and PPII bias compared to experimental results. Simulated curves (reproduced from Figure 5) are compared to experimental mean R_h from the IDPs in Table S1. Open circles in panel **A)** used the coil library scale to calculate f_{PPII}. Fractional ΔR_h for each IDP was determined by (experimental mean R_h – (2.16Å·$N^{0.518}$ + 0.25·|Q_{net}| - 0.27·$N^{0.5}$)) / (2.16Å·$N^{0.518}$ + 0.25·|Q_{net}| - 0.27·$N^{0.5}$), where 2.16Å·$N^{0.518}$ is the simulated ensemble size without an artificially applied PPII or α bias and 0.25·|Q_{net}| - 0.27·$N^{0.5}$ accounts for net charge effects. Open circles in panel **B)** used the IDP scale to calculate f_{PPII}. Fractional ΔR_h for each IDP was determined by (experimental mean R_h – (2.16Å·$N^{0.518}$ + 0.25·|Q_{net}| - 0.21·$N^{0.5}$)) / (2.16Å·$N^{0.518}$ + 0.25·|Q_{net}| - 0.21·$N^{0.5}$), where 2.16Å·$N^{0.518}$ is the simulated ensemble size without an artificially applied PPII or α bias and 0.25·|Q_{net}| - 0.21·$N^{0.5}$ accounts for net charge effects.

Supporting References

(1) English, L. R.; Tilton, E. C.; Ricard, B. J.; Whitten, S. T. Intrinsic α Helix Propensities Compact Hydrodynamic Radii in Intrinsically Disordered Proteins. *Proteins* **2017**, *85* (2), 296–311.

(2) Marsh, J. A.; Forman-Kay, J. D. Sequence Determinants of Compaction in Intrinsically Disordered Proteins. *Biophys. J.* **2010**, *98* (10), 2383–2390.

(3) Elam, W. A.; Schrank, T. P.; Campagnolo, A. J.; Hilser, V. J. Evolutionary Conservation of the Polyproline II Conformation Surrounding Intrinsically Disordered Phosphorylation Sites. *Protein Sci.* **2013**, *22* (4), 405–417.

(4) Jha, A. K.; Colubri, A.; Zaman, M. H.; Koide, S.; Sosnick, T. R.; Freed, K. F. Helix, Sheet, and Polyproline II Frequencies and Strong Nearest Neighbor Effects in a Restricted Coil Library. *Biochemistry* **2005**, *44* (28), 9691–9702.

(5) Shi, Z.; Chen, K.; Liu, Z.; Ng, A.; Bracken, W. C.; Kallenbach, N. R. Polyproline II Propensities from GGXGG Peptides Reveal an Anticorrelation with Beta-Sheet Scales. *Proc. Natl. Acad. Sci. U. S. A.* **2005**, *102* (50), 17964–17968.

(6) Creamer, T. P. Left-Handed Polyproline II Helix Formation Is (Very) Locally Driven. *Proteins* **1998**, *33* (2), 218–226.

(7) Langridge, T. D.; Tarver, M. J.; Whitten, S. T. Temperature Effects on the Hydrodynamic Radius of the Intrinsically Disordered N-Terminal Region of the P53 Protein. *Proteins* **2014**, *82* (4), 668–678.

(8) Whitten, S. T.; Yang, H.-W.; Fox, R. O.; Hilser, V. J. Exploring the Impact of Polyproline II (PII) Conformational Bias on the Binding of Peptides to the SEM-5 SH3 Domain. *Protein Sci. Publ. Protein Soc.* **2008**, *17* (7), 1200–1211.

(9) Tomasso, M. E.; Tarver, M. J.; Devarajan, D.; Whitten, S. T. Hydrodynamic Radii of Intrinsically Disordered Proteins Determined from Experimental Polyproline II Propensities. *PLoS Comput. Biol.* **2016**, *12* (1), e1004686.